THE BULLETIN OF OKAYAMA UNIVERSITY OF SCIENCE No. 44 A pp. 133-140(2008)

A Consideration of Filtration Flux in Cross-Flow Microfiltration for Dilute Suspensions of Submicron Particles

Toshiro MIYAHARA and Naoki NAGATANI

Department of Applied Chemistry and Biotechnology,
Faculty of Engineering,
Okayama University of Science,
1-1, Ridai-cho, Okayama 700-0005, Japan

(Received September 8, 2008; accepted November 7, 2008)

Experiments were performed to study the characteristics of filtration flux in cross-flow microfiltration for dilute suspensions of submicron particles. The flux decline from the initial value to the steady state value is considered using a semi-theoretical unsteady state model for the permeate flux developed by Makardij *et al.*[1] for the flux in cross-flow microfiltration and ultrafiltration in relatively high solids contents. As a result, the model describes well the flux decline in cross-flow microfiltration for dilute suspensions of submicron particles except for the beginning of filtration period. It is also found that the flux values at the steady state can be well estimated using the model.

Keywords: cross-flow microfiltration; submicron particle; dilute suspension; solid liquid separation; flux decline.

1. Introduction

Cross-flow microfiltration is a relatively new process of growing importance which allows separation of small particles at higher permeate fluxes than conventional dead-end filtration. In the process, the fluid flows tangentially to the membrane surface: the shearing action of the fluid prevents the development of thick filter cakes at the membrane surface. Uses for this technology include clarification of fruit juices and concentration of materials such as fermentation broths, especially a solid-liquid separation technique in the downstream processing of bio-products from microbial sources.[2,3] This technology has also been applied to the treatment of industrial waste water; especially the separation of oily water.[4] While it is generally accepted that the shear stress associated with tangential flow is responsible for keeping cake growth to a minimum, the shear action is not clearly defined.[5, 6, 7, 8, 9,10,11] In practice, flux decline is observed over time, and permeate flux with the cake and membrane resistances being time dependent has usually been evaluated from Darcy's law. In this case, there are complicated circumstances because we must know the various resistances such as membrane resistance, concentration polarization resistance and the resistance of the cake layer, respectively in advance. Recently, Makardij *et al.*[1] have proposed a simple but effective model for cross-flow microfiltration and ultrafiltration, in which it was assumed that the initial flux would start to drop upon the start of the membrane operation due to concentration polarization resistance and the flux will then decline gradually due to the net effects of deposition on or into the membrane and deposit removal due to the cross-flow of the retentate, and applied the model to cases of relatively high feed solids contents: 6, 8 and 10 kg/m^3. They concluded that this simple model could form the basis for further research and advanced analysis.

In the present study, the model proposed by Makardij *et al.*[1] is applied to the flux decline in cross-flow microfiltration of dilute suspensions of submicron particles: 0.15 to 1 kg/m^3. As a result, it is found that it is possible to evaluate the flux decline except for the beginning of filtration period and also steady state values of permeate flux can be well predicted by the model.

2. Experimental

A schematic diagram of the cross-flow microfiltration system is shown in **Fig. 1**. It is comprised of a feed circulation system, a cross-flow filtration module and a computer system to measure the filtrate. **Figure 2** shows the assembly of the module. The module was constructed with three assemblies (A, B and C). The feed solution was pumped into the flow channel through the A and B assemblies. The dimensions of the flow channel were: depth 5 mm, width 5 cm and length 35 cm. A nuclepore membrane with a pore size of 0.2 μm (Polycarbonate, Nomura Micro Science Co., Ltd.) was set on the bronze support of a porous plate. The effective membrane area for the filtrate was 75 cm^2. The cross-flow velocity was varied from 0.28 to 0.83 m/s. The filtration pressure was

varied in the range of 50 – 120 kPa. The concentration of the suspensions ranged from 0.15 kg/m^3 to 1.0 kg/m^3. Three kinds of PMMA particles (0.19 – 0.86 μm in diameter) as shown in **Table 1** were employed as model particles. The particle sizes in Table 1 were evaluated using a particle size instrument (model ELS-80R, Otsuka Electronics Co.). Pure water obtained by reverse osmosis instrument (Elix10, Japan Millipore Co., Ltd.) was used. The working volume of feed tank was 35 ℓ and 2 g of Sodium Hexametaphosphate was added to the feed solution in order to prevent the aggregation between particles under the agitation by magnetic stirrer and the irradiation of ultrasonic wave.

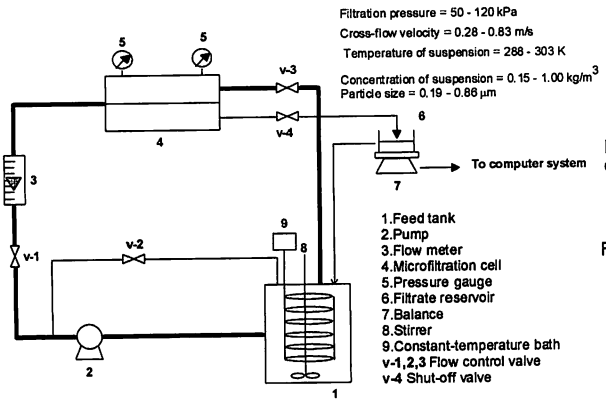

Fig. 1 Schematic diagram of experimental apparatus

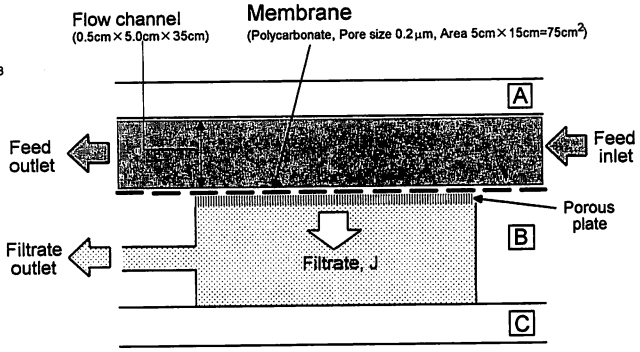

Fig. 2 Cross-flow microfiltration module

Table 1 Characteristics of particles employed in this study

Particle	Volumetric mean diameter [μm]	Density [kg/m^3]	Remarks
MP-1451	0.19	1183	Polymethyl methacrylate(PMMA)
MP-1000	0.48		
MP-1400	0.86		

These particles were purchased from Soken Chemical Co., Ltd.

3. Results and Discussion

3.1 The model developed by Makardij *et al.*[1]

Usually, flux decline for cross-flow microfiltration or ultrafiltration has been evaluated by Darcy's law written as follows

$$J = \frac{\Delta P}{\mu\left(R_{\mathrm{m}} + R_{\mathrm{cp}} + R_{\mathrm{c}}\right)} \tag{1}$$

where J is the permeate flux, ΔP the filtration pressure and R_{m}, R_{cp} and R_{c} are the membrane resistance, the concentration polarization resistance and the resistance of the cake layer, respectively. When we use this equation, we need three kinds of resistances mentioned above in advance.

For this reason, Makardij *et al.*[1] has developed a simple but effective model for cross-flow microfiltration and ultrafiltraion. In the development, they assumed that the initial flux would start to drop upon the start of the membrane operation due to concentration polarization resistance. The flux will then decline gradually due to the net effect of deposition on or into the membrane and deposit removal due to the cross-flow of the retentate, that is, the rate of flux decline is equal to the rate at which solids or solutes are brought to the membrane surface

minus the rate at which deposit is removed from the membrane. In the mathematical form, the following equation can be written as

$$-\frac{dJ}{dt} = k_1 CJ - k_2 Re^n \tag{2}$$

where C is the feed concentration, k_1 is the rate constant for flux decline, k_2 is the rate constant for deposit removal from the membrane and the Reynolds number $Re = du\rho/\mu$. Where ρ is the density, u is the retentate cross-flow velocity, μ is viscosity of the retentate. In cases where channel through which the feed fluid flows in is not of circular cross section, d is recommended to be the hydraulic mean diameter, which is calculated by dividing four times the cross sectional area of the flow by the wetted perimeter. The power n needs to be established experimentally. Hence, Equation (2) defines the local permeate flux at any position in the membrane. Now, Equation (2) can be rewritten as follows

$$-\frac{dJ}{dt} = a(J-b) \tag{3}$$

where $a = k_1 C$ and $b = \frac{k_2}{k_1 C} Re^n$.

Integrating Equation (3) under the initial condition of $J = J_0$ at $t = 0$ gives

$$J - b = (J_0 - b)e^{-at} \tag{4}$$

Equation (4) shows an exponential decay of the permeate flux with both time and concentration. It shows that as $t \to \infty$, J approaches the steady flux J_s. Then b becomes J_s. Therefore, Equation (4) is rewritten as follows.

$$J - J_s = (J_0 - J_s)e^{-at} \tag{5}$$

As described above, in Equation (5), $J_s = b$, then

$$J_s = \frac{k_2}{k_1 C} Re^n \tag{6}$$

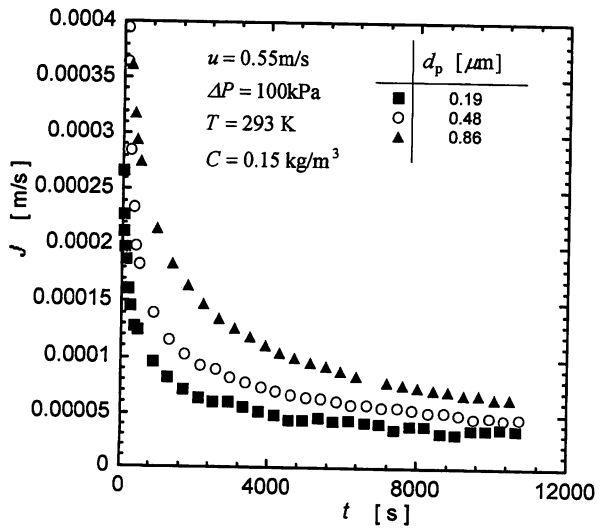

Fig. 3 Time course of filtration flux

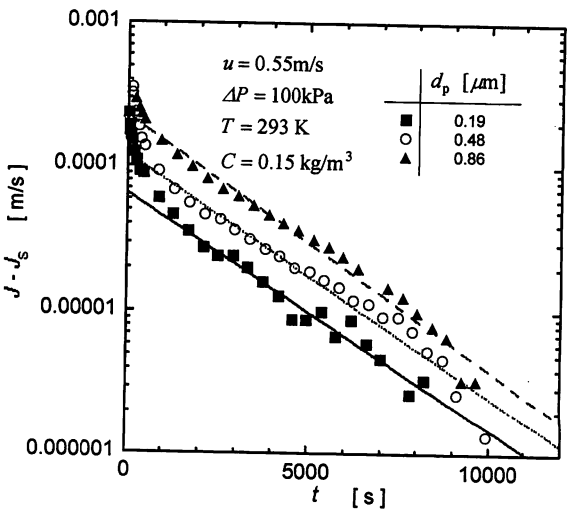

Fig. 4 Semi-log plot of $(J - J_s)$ against time

3.2 Time course of filtration flux

Figure 3 shows the time course of filtration flux. The experimental data are re-plotted as semi-log plot as shown in **Fig. 4** to evaluate the values of initial flux J_0 and the flux decline coefficient k_1.

The linear fit, shown in Fig. 4, is a support to the model suggested except for the beginning of the filtration period. It is suggested that the deviation from the linear fit occurs at the beginning of the filtration period due to the fact that the membrane surface at that time has not been completely covered with the cake layer instantaneously. Also it is expected that some deviation from the linear fit occurs at the end of the filtration period due to the fact that the flux at that time has not completely reached steady state. Based on Equation (5), k_1C is the slope of the line in Fig. 4, while the initial flux J_0 is evaluated from the intercept of the line. The value of k_2 is calculated from the log-log plot of J_s vs. Re shown in **Fig. 5**. From the same graph, we can obtain an approximate value of the exponent n of around 0.2 in all experimental conditions employed in this study. The values of k_1, k_2, J_0, J_s and n are listed in **Tables 2, 3** and **4** for each submicron particle employed, together with the experimental conditions in this study.

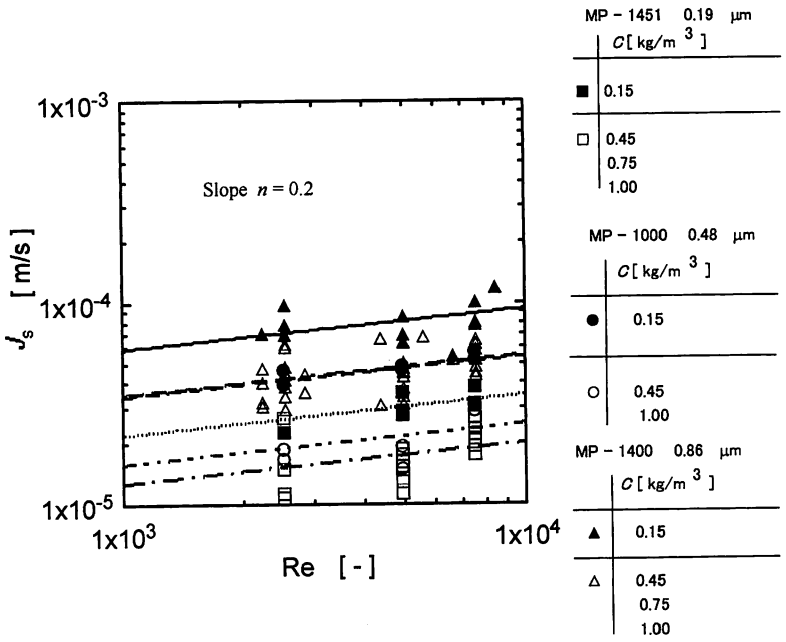

Fig. 5 Log-log plot of J_s against Re

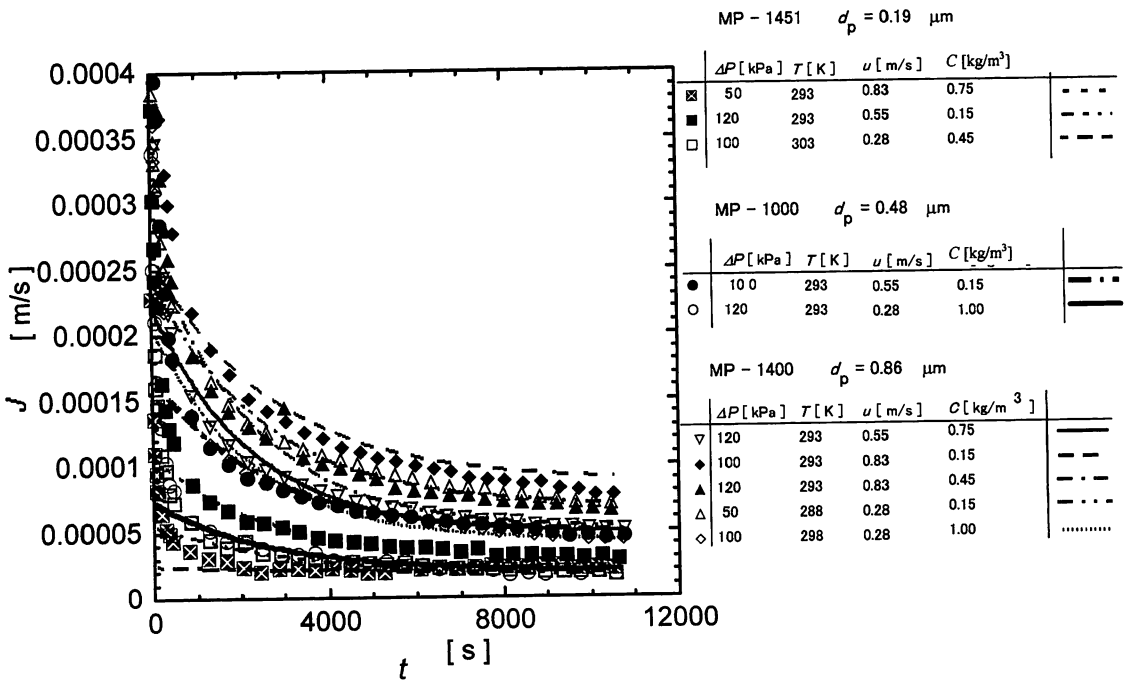

Fig. 6 Comparison of experimental flux decline data with calculated ones

Table 2 Parameters in the model proposed by Makardij *et al.*[1] in each condition for MP-1451 (d_p=0.19 μm)

ΔP [kPa]	T [K]	u [m/s]	C [kg/m^3]	ρ [kg/m^3]	μ [Pa·s]	$k_1 \times 10^4$ [m^3/kg·s]	$k_2 \times 10^{10}$ [m/s^2]	$J_0 \times 10^5$ [m/s]	$Re \times 10^{-3}$ [-]	n [-]	$J_s \times 10^5$ [m/s]
50	293	0.28	1	998	0.00101	4.26	9.52	3.67	2.52	0.2	1.07
50			0.75			4.12	7.29	3.79			1.13
50			0.45			7.49	10.3	5.00			1.47
50			0.15			22.4	15.9	7.24			2.27
50		0.55	1			3.15	7.65	3.22	4.94		1.33
50			0.75			4.89	8.51	3.35			1.27
50			0.45			8.98	12.8	4.42			1.73
50			0.15			25.9	19.3	8.32			2.73
50		0.83	1			1.74	6.43	2.62	7.46		2.20
50			0.75			2.59	6.75	2.60			2.07
50			0.45			5.78	10.2	3.34			2.33
50			0.15			24.9	19.7	6.07			3.13
100		0.28	0.45			7.29	10.1	4.45	2.52		1.47
100		0.55	1			2.14	4.41	2.92	4.94		1.13
100			0.75			3.19	6.67	3.76			1.53
100			0.45			6.78	9.63	5.36			1.73
100			0.15			25.3	24.5	10.1			3.53
100		0.83	0.45			7.38	9.65	3.98	7.46		1.73
120		0.28				7.02	17.6	6.43	2.52		2.67
120		0.55	1			3.50	8.49	3.67	4.94		1.33
120			0.75			5.60	12.3	5.02			1.60
120			0.45			8.67	13.3	6.30			1.87
120			0.15			26.5	20.8	10.9			2.87
120		0.83	1			3.95	12.8	4.60	7.46		1.93
120			0.75			6.28	18.4	6.31			2.33
120			0.45			11.0	22.1	7.98			2.67
120			0.15			24.4	23.4	12.3			3.80
100	303	0.28	0.45	910	0.000802	6.44	9.84	5.60	2.89	0.2	1.67
100		0.55				9.27	15.8	6.27	5.67		2.13
100		0.83				9.78	23.0	5.76	8.56		3.20

Table 3 Parameters in the model proposed by Makardij *et al.*[1] in each condition for MP-1000 (d_p=0.48 μm)

ΔP [kPa]	T [K]	u [m/s]	C [kg/m^3]	ρ [kg/m^3]	μ [Pa·s]	$k_1 \times 10^4$ [m^3/kg·s]	$k_2 \times 10^{10}$ [m/s^2]	$J_0 \times 10^5$ [m/s]	$Re \times 10^{-3}$ [-]	n [-]	$J_s \times 10^5$ [m/s]
50	293	0.28	0.45	998	0.00101	9.56	16.8	6.38	2.52	0.2	1.87
		0.55				5.58	6.73	3.97	4.94		1.47
		0.83				4.00	9.29	5.23	7.46		3.07
100		0.28	0.15			25.0	30.8	14.7	2.52		3.93
		0.55				25.8	32.5	16.8	4.94		4.60
		0.83				24.5	35.0	16.7	7.46		5.67
120		0.28	1			3.77	13.2	7.40	2.52		1.67
		0.55				3.81	13.4	7.55	4.94		1.93
		0.83				3.52	17.0	4.77	7.46		2.87
		0.28	0.15			31.5	45.3	23.1	2.52		4.60
		0.55				28.2	37.6	24.2	4.94		4.87
		0.83				30.7	39.7	23.1	7.46		5.13

Table 4 Parameters in the model proposed by Makardij *et al.*[1] in each condition for MP-1400 (d_p=0.86 μm)

ΔP [kPa]	T [K]	u [m/s]	C [kg/m^3]	ρ [kg/m^3]	μ [Pa·s]	$k_1 \times 10^4$ [m^3/kg·s]	$k_2 \times 10^{10}$ [m/s^2]	$J_0 \times 10^5$ [m/s]	$Re \times 10^{-3}$ [-]	n [-]	$J_s \times 10^5$ [m/s]
50	293	0.28	1	998	0.00101	3.89	23.8	11.1	2.54	0.2	2.93
			0.75			4.17	22.2	11.3			3.40
			0.45			7.29	30.7	15.2			4.13
			0.15			25.8	55.4	24.9			6.87
		0.55	1			4.08	23.3	10.7	4.98		3.13
			0.75			5.18	26.4	11.5			3.75
			0.45			7.80	27.3	14.5			4.27
			0.15			23.3	44.1	23.6			6.93
		0.83	1			3.99	29.0	9.39	7.52		4.33
			0.75			5.70	32.1	11.9			4.47
			0.45			9.34	38.1	14.3			5.40
			0.15			25.4	51.1	25.8			8.00
100		0.28	1			4.12	32.7	15.4	2.54		3.80
			0.75			5.13	35.8	19.3			4.47
			0.45			10.3	57.8	25.9			6.00
			0.15			26.0	63.0	34.8			7.73
		0.55	1			5.63	34.9	23.8	4.98		3.40
			0.75			5.86	37.4	20.5			4.67
			0.45			8.37	31.1	21.1			4.53
			0.15			30.4	53.2	34.3			6.40
		0.83	1			4.51	38.9	15.1	7.52		5.13
			0.75			5.03	30.4	14.1			4.80
			0.45			10.5	48.5	22.1			6.13
			0.15			24.2	47.2	25.9			7.73
120		0.28	1			3.42	31.4	15.6	2.54		4.40
			0.75			4.64	34.3	17.0			4.73
			0.45			8.64	49.7	22.8			6.13
			0.15			24.1	73.2	35.4			9.73
		0.55	1			4.24	34.5	17.9	4.98		4.47
			0.75			5.87	40.1	22.2			5.00
			0.45			8.45	43.9	23.2			6.33
			0.15			30.9	72.0	46.6			8.53
		0.83	1			4.04	32.1	15.8	7.52		4.73
			0.75			5.15	37.6	19.5			5.80
			0.45			9.61	47.4	26.7			6.53
			0.15			29.6	75.6	44.6			10.1
50	288	0.28	1	999	0.00114	4.37	28.0	11.9	2.23	0.2	3.00
			0.75			4.39	22.5	10.7			3.20
			0.45			10.0	44.9	18.0			4.67
			0.15			25.9	58.3	24.2			7.00
		0.55	0.75			4.29	18.4	9.75	4.39		3.07
50	298	0.28	0.75	997	0.00089	4.90	26.4	13.3	2.85	0.2	3.53
100		0.55	0.45			8.79	47.4	23.5	5.60		6.73
120		0.83	0.15			33.3	97.7	47.7	8.45		11.9
100		0.28	1			4.44	39.8	20.6	2.85		4.40
50	288	0.83	0.15	999	0.00114	27.2	38.3	22.9	6.62	0.2	5.47
120		0.55	0.45			9.27	51.4	24.4	4.39		6.60
100		0.83	0.75			5.67	37.6	17.1	6.62		5.13
100		0.28	1			4.29	36.7	16.6	2.23		4.00

3.3 Consideration of filtration flux for dilute suspensions of submicron particles

From experimental results employed in the present study, we found that filtration flux increases with increasing filtration pressure and cross-flow velocity and with decreasing concentration of suspension and liquid viscosity leading to high temperature of the liquid.

Examining the values of k_1 and k_2 can determine whether the membrane tend to foul easily or be cleaned easily. From Tables 2, 3 and 4, roughly, high values of k_1 indicates membrane high tendency to foul, while high values of k_2 indicates the easiness of cleaning.

Theoretical values of permeate flux are calculated using the values of k_1, k_2, J_0 and n shown in Tables 2, 3 and 4. The measured and predicted fluxes are shown in **Fig. 6** for some flux decline data. The general trend of the flux decline measured approximately is in an agreement with that predicted, except for the beginning of filtration period. Various curves in the figure are calculated ones.

3.4 Permeate flux value at steady state

The permeate flux value at steady state is important in practical operation of cross-flow microfiltration. The flux values at steady state can be evaluated by Equation (6) using k_1, k_2, C and n shown in Tables 2, 3, and 4. This argument could be confirmed from the results in Fig. 6.

4. Concluding Remarks

The model proposed by Makardij *et al.*[1] for the flux in cross-flow microfiltration and ultrafiltration in relatively high solids contents is examined for the characteristics of filtration fluxs in cross-flow microfiltration for dilute suspensions of submicron particles. As a result, the following conclusions were drawn:

1) The filtration flux decline data can be well described by the model proposed by Makardij *et al.*[1] except for the beginning of filtration period.
2) The flux values at steady state are predicted by the model.

Notation

C = concentration of suspension, kg/m^3
d = hydraulic mean diameter, m
d_P = particle diameter, m
J = filtration flux, m/s
J_s = filtration flux at steady state, m/s
J_0 = initial filtration flux, m/s
k_1 = rate constant for flux decline, m^3/(kg·s)
k_2 = rate constant for deposit removal, m/s^2
n = exponent
Re =Reynolds number
R_c = resistance of cake layer, 1/m
R_{cp} = resistance of concentration polarization, 1/m
R_m = resistance of clean membrane, 1/m
t = filtration time, s
u = cross-flow velocity, m/s
ΔP = filtration pressure, Pa
ρ = retentate density, kg/m^3
μ = retentate viscosity, Pa·s

References

1 Makardij, A. A., Faird, M. M. and Chen, X.-D.; " A simple and effective model for cross-flow microfiltration and ultrafiltration," *Can. J. Chem. Eng.*, **80**, 28-36 (2002)
2 Nakanishi, K. and Tanaka, T.; "Crossflow filtration of microbial suspension," *Nippon ShokuhinKogyo Gakkaishi*, **41**, 578-584 (1994)
3 Tanaka, T., Abe, K., Asakawa, H., Yoshida, H. and Nakanishi, K. (1994); "Filtration characteristics and structure of cake in crossflow filtration of bacterial suspension," *J. Fermentation and Bioengineering*, **78**, 455-461 (1994)
4 Mueller, J., Cen, Y.-W. and Davies, R. H.; "Crossflow microfiltration of oily water," *J. Membrane Sci*, **129**, 221-235 (1997)
5 Blake, N. J., Cumming, I. W. and Streat, M.; "Prediction of steady state crossflow filtration using a force balance model," *J. Membrane Sci*, **68**, 205-216 (1992)
6 Nassehi, V.; "Modeling of combined Navier-Stokes and Darcy flows in crossflow membrane filtration," *Chem. Eng. Sci.*, **53**, 1253-1265 (1998)

7 Chellam, S. and Wiesner, M. R.; "Evaluation of crossflow filtration models based on sheared-induced diffusion and particle adhesion: Complications induced by feed suspension polydispersivity," *J. Membrane Sci.*, **138**, 83-97 (1998)
8 Hwang, J., Chang, D.-J. and Chen, C.H.; "Steady state permeate flux for particle cross-flow filtration," *Chem. Eng. J.*, **61**, 171-178 (1997)
9 Iritani, E., Hayashi, T. and Murase, T.; "Analysis of filtration mechanism of crossflow upward and downward ultrafiltration," *J. Chem. Eng. Japan.*, **24**, 39-44 (1991)
10 Stamatakis, K. and Tien, C.; "A simple model of cross-flow filtration based on particle adhesion," *AIChEJ.*, **39**, 1292-1302 (1993)
11 Wang, W., Jia, X. and Davies, G. A.; "A theoretical study of transient crossflow filtration using force balance analysis," *Chem. Eng. J.*, **60**, 55-62 (1995)